Research Article

Cancer Prevention Research

Genetic Manipulation of Homologous Recombination *In Vivo* Attenuates Intestinal Tumorigenesis

Michael A. McIlhatton[1], Kevin Murnan[1], Daniel Carson[2], Gregory P. Boivin[3], Carlo M. Croce[1], and Joanna Groden[1]

Abstract

Although disruption of DNA repair capacity is unquestionably associated with cancer susceptibility in humans and model organisms, it remains unclear if the inherent tumor phenotypes of DNA repair deficiency syndromes can be regulated by manipulating DNA repair pathways. Loss-of-function mutations in *BLM*, a member of the *RecQ* helicase family, cause Bloom's syndrome (BS), a rare, recessive genetic disorder that predisposes to many types of cancer. BLM functions in many aspects of DNA homeostasis, including the suppression of homologous recombination (HR) in somatic cells. We investigated whether BLM overexpression, in contrast with loss-of-function mutations, attenuated the intestinal tumor phenotypes of $Apc^{Min/+}$ and $Apc^{Min/+}$;$Msh2^{-/-}$ mice, animal models of familial adenomatous polyposis coli (FAP). We constructed a transgenic mouse line expressing human BLM (*BLM-Tg*) and crossed it onto both backgrounds. *BLM-Tg* decreased adenoma incidence in a dose-dependent manner in our $Apc^{Min/+}$ model of FAP, although levels of GIN were unaffected and concomitantly increased animal survival over 50%. It did not reduce intestinal tumorigenesis in $Apc^{Min/+}$;$Msh2^{-/-}$ mice. We used the pink-eyed unstable (p^{un}) mouse model to demonstrate that increasing BLM dosage *in vivo* lowered endogenous levels of HR by 2-fold. Our data suggest that attenuation of the *Min* phenotype is achieved through a direct effect of *BLM-Tg* on the HR repair pathway. These findings demonstrate that HR can be manipulated *in vivo* to modulate tumor formation at the organismal level. Our data suggest that lowering HR frequencies may have positive therapeutic outcomes in the context of specific hereditary cancer predisposition syndromes, exemplified by FAP. *Cancer Prev Res; 8(7); 650–6. ©2015 AACR.*

Downloaded from http://aacrjournals.org/cancerpreventionresearch/article-pdf/8/7/650/2254579/650.pdf by guest on 20 July 2024

Introduction

The RecQ-like helicase family members *WRN*, *BLM*, and *RECQL4* are linked to human genetic diseases characterized by genome instability, premature aging, and cancer predisposition (1, 2). BLM is a structure-specific helicase with 3′-5′ directionality which is involved in DNA double-strand break (DSB) repair (3). BLM functions in many aspects of DNA homeostasis, including the restart/repair of stalled and collapsed replication forks during DNA replication, repair of interstrand cross-links, and resolution of Holliday junctions (4–6). While it is accepted that BLM promotes resolution of Holliday intermediates by dissolution, thus suppressing crossovers, the role of *BLM* in homologous recombination (HR) is more complex than merely this late stage role. BLM also disrupts formation of RAD51-ssDNA filaments, leading to disruption of D-loops and thus suppression of HR at earlier stages (7). BLM-deficient cells have an approximate 10-fold increase in the number of sister chromatid exchanges (SCE) caused by inappropriate HR between sister chromatids at the S or G_2 phases of the cell cycle (8). Bloom's syndrome (BS) is a rare, recessive genetic disorder that is caused by loss-of-function mutations in the *BLM* gene (9). BS patients have a predisposition to develop many types of cancer, presenting with a mean age of 24 years at diagnosis.

Several lines of evidence indicate that *Blm* dosage is critical for controlling the onset of tumorigenesis in mice. Mouse models demonstrate that chromosomal instability directly correlates with the levels of Blm; as Blm decreases, genomic instability and tumor burden increase (10–12). In addition, haploinsufficiency for *Blm* on the *C57Bl-6J* $Apc^{Min/+}$ background increases spontaneous adenoma formation and dysplasia (11). Genomic analyses of $Apc^{Min/+}$;$Blm^{Cin/+}$ mice indicate that increased adenoma formation is a direct consequence of reduced Blm levels and an increase in somatic recombination. This, in turn, facilitates loss of the wild-type *Apc* allele by interchromosomal recombination and leads to increased loss-of-heterozygosity (LOH). In humans, similar conclusions have been reached about carriers of specific *BLM* mutations and their resulting susceptibilities to colorectal cancer (13).

Familial adenomatous polyposis coli (FAP) is a hereditary human cancer predisposition syndrome characterized by the growth of hundreds to thousands of small adenomatous polyps throughout the colon (reviewed in ref. 14). FAP requires the inheritance of a mutated allele of the adenomatous polyposis coli (*APC*) gene (15). Depending on the nature of the inherited germline allele, second-hit inactivation of the wild-type allele is achieved either by LOH of the *APC* locus or intragenic mutation of

[1]Department of Molecular Virology, Immunology and Medical Genetics, The Ohio State University, Columbus, Ohio. [2]Clermont College, University of Cincinnati, Batavia, Ohio. [3]Department of Pathology, Boonshoft School of Medicine, Wright State University, Dayton, Ohio.

Note: Supplementary data for this article are available at Cancer Prevention Research Online (http://cancerprevres.aacrjournals.org/).

Corresponding Author: Joanna Groden, The Ohio State University, BRT, Room 986, 460 West 12th Avenue, Columbus, OH 43210. Phone: 614-685-4685; Fax: 614-292-4499; E-mail: joanna.groden@osumc.edu

doi: 10.1158/1940-6207.CAPR-15-0001-T

©2015 American Association for Cancer Research.

the APC gene (16). APC is also inactivated by intragenic mutation in 70% to 80% of individuals with sporadic colorectal cancer (14).

Given the demonstrated relationship between low or absent expression levels of BLM and cancer, we investigated whether constitutive overexpression of BLM modulated adenoma formation in the $Apc^{Min/+}$ mouse model of FAP (17). We hypothesized that if halving *Blm* gene dosage increased predisposition to tumorigenesis, overexpression would conversely decrease tumor susceptibility. Understanding the mechanism by which BLM attenuates tumor susceptibility will aid our fundamental understanding of its roles in maintaining genomic stability and suggest new strategies for cancer prevention involving direct regulation of DNA repair pathways. Our data suggest that levels of specific DNA repair proteins may be titrated to achieve positive therapeutic outcomes in the context of specific hereditary cancer syndromes, exemplified by FAP.

Materials and Methods

Generation of the transgenic mouse line expressing BLM

The procedure is outlined below. The human *BLM* cDNA was amplified from plasmid *pJK1* and cloned into the *TA-vector* (Promega). The construct was sequenced and verified. A 0.44 kb fragment, corresponding to the phosphoglycerate kinase (*PGK*) promoter, was cloned in to the 5′ end of the *BLM* cDNA. The *PGK-BLM* cDNA fragment was then cloned into the vector *pOPRSVICat*, containing a synthetic intron and the HSV thymidine kinase (*TK*) polyadenylation signal. The *PGK-BLMcDNA-p(A)* fragment was removed by restriction digestion from the vector, purified, and introduced into *C57Bl-6J* oocytes by pronuclear injection. Founder lines were generated and initially screened for the presence of the transgene by Southern blotting. A probe corresponding to the 3′ end of the *BLM* cDNA was used. Once germline transmission had been established, transgenic animals were routinely identified using PCR.

Generation of mice lines and genotyping

$Apc^{Min/+}$ mice were originally obtained from The Jackson Laboratories (stock: 002020; strain: *C57BL/6J-*Apc^{Min}*/J*). $Blm^{Cin/+}$ mice have been previously reported (11). The pink-eyed unstable mouse model (18) was a gift from Dr. A.J.R. Bishop, University of Texas Health Science Center at San Antonio. Heterozygous $Msh2^{+/-}$ mice (19) were obtained from the laboratory of Dr. Winfried Edelmann, Albert Einstein College of Medicine, New York. $Apc^{Min/+}$, $Blm^{Cin/+}$, $Msh2^{+/-}$, and *BLM-Tg* lines were intercrossed to generate mice of the required genotypes, all on congenic *C57BL/6J* backgrounds. Animals were bred in a barrier facility and were maintained according to the NIH animal care and use guidelines. Both male and female mice were included in experimental study groups for subsequent analyses. All experiments involving animals received prior approval from the OSU Institutional Animal Care and Use Committee. $Apc^{Min/+}$, $Blm^{Cin/+}$ and $Msh2^{+/-}$ mice were genotyped as described previously (11, 19).

Genotyping *BLM-Tg* mice

Mice were genotyped as follows: primers hBE3F (5′-TAT GCA CTA CCC AAA ACA CAC C-3′; forward) and hBE3R (5′-TCA GTC AAA TCT ATT TGC TCG C-3′; reverse) were used in a PCR reaction to amplify a 310 bp product from exon 3 of human *BLM*. Primers HMGAPF (5′-GAC ATC AAG AAG GTG GTG AAG-3′; forward) and HMGAPR (5′-CCA GGA AAT GAG CTT GAC AAA G-3′; reverse) were used to amplify a 171 bp product from mouse Gapdh as an internal positive control. PCR reactions were performed with standard *Taq* polymerase.

qPCR to determine allelic status of *BLM-Tg*

Primers BLM09F (5′-TGG TGC GGA AGT GAT TTC AGT A-3′; forward) and BLM12R (5′-TTT ATA GGC TTC GGT GGA GC-3′) were used to amplify a 396 bp amplicon from the 3′ end of the *BLM* cDNA. The SYBR Green PCR Master Mix (Invitrogen) was used for all qPCR reactions. Purified DNAs from *BLM-Tg* mice were used as templates. Reactions were performed with a series of dilutions of each template. Cycle threshold (C_t) was plotted against $\log_{10}$[DNA] and used to identify hemizygous ($BLM^{+/T}$) and homozygous ($BLM^{T/T}$) transgenic mice. All qPCR reactions were run in triplicate and repeated at least twice.

Animal dissection

Mice were euthanized at 16 weeks by CO_2 inhalation, followed by cervical dislocation. Intestines were removed, rinsed in PBS, and cut into sections corresponding to the duodenum, jejunum, ileum, cecum, and colon (large intestine). Tissues were opened longitudinally, washed twice in PBS, and examined under a dissecting microscope. Gross numbers of adenomas/intestinal polyps were counted. Tissues were fixed in 10% formalin overnight, blocked in paraffin, sectioned, and stained with hematoxylin and eosin. Slides were evaluated to confirm tumors and determine gastrointestinal neoplasia (GIN). The criteria for GIN are as described previously (20).

Ethics statement

All experiments involving mice received prior approval from The Ohio State University Institutional Animal Care and Use Committee (IACUC), OLAW Assurance #A3261-01. Animal work was conducted in accordance with the established criteria of our animal use protocol, #2012A00000021, approved by IACUC. Mice were observed on a daily basis for predetermined criteria necessitating removal and euthanasia. Decisions to remove animals were made in conjunction with the veterinarian staff of our animal facility. Mice were euthanized by CO_2 inhalation, followed by cervical dislocation.

Dissection of the RPE/scoring reversion events

These have been described previously (18).

Statistical analysis

All statistical analyses were performed with Prism 6.1.

Results

BLM expression rescues the embryonic lethality of the Blm^{Cin} knockout mouse

A transgenic mouse was generated that expressed human BLM on a congenic *C57Bl-6J* background, hereafter designated *BLM-Tg*. qPCR was used to establish the allelic status of the *BLM* transgene in sibling mice bred from the established colony (Supplementary Fig. S1). Protein expression levels correlated with the allelic status of the transgene; homozygous ($BLM^{T/T}$) mice expressed approximately twice as much BLM as hemizygous ($BLM^{+/T}$) mice. The *BLM-Tg* also rescued the embryonic lethality of the conventional $Blm^{Cin/Cin}$ knockout mouse (11). Mating of $BLM^{+/T}$;$Blm^{Cin/+}$ animals yielded $BLM^{+/T}$;$Blm^{Cin/Cin}$ mice at normal Mendelian ratios.

Downloaded from http://aacrjournals.org/cancerpreventionresearch/article-pdf/8/7/650/2254579/650.pdf by guest on 20 July 2024

Long-term expression of BLM for over 24 months had no apparent deleterious effects on animal health. *BLM-Tg* mice ($n = 3$) were subjected to full necropsy and phenotypic analyses. No overt phenotypic abnormalities were detected; only age- or strain-related lesions were observed (data not shown). Tumors were not apparent in any tissue at necropsy, and there was no evidence of architectural destruction or invasion which would suggest neoplastic transformation.

Transgenic expression of BLM reduces adenoma numbers in $Apc^{Min/+}$ mice

The *BLM-Tg* line was crossed to $Apc^{Min/+}$ mice, also on a *C57Bl-6J* background. Animals were maintained in a barrier environment, and four different groups of litter mates were generated: (i) $Apc^{Min/+}$, (ii) $Apc^{Min/+};BLM^{+/T}$, (iii) $Apc^{Min/+};BLM^{T/T}$, and (iv) $BLM^{+/T}$ and/or wild-type mice. Mice were euthanized after 16 weeks and gross intestinal adenomas were counted with a dissecting microscope to differentiate adenomas in the duodenum, jejunum, ileum, cecum, and colon. Pathology studies confirmed and categorized adenomas as low- or high-grade and scored GIN according to the criteria of Boivin and colleagues as an early marker for neoplasia (20).

BLM-Tg significantly reduced gross numbers of intestinal adenomas in $Apc^{Min/+}$ litter mates (Fig. 1A; Table 1). $Apc^{Min/+}$ mice developed a mean of 46.44 ± 11.42 adenomas, compared with 24.44 ± 8.22 for $Apc^{Min/+};BLM^{+/T}$ and 17.24 ± 8.26 for $Apc^{Min/+};BLM^{T/T}$ mice ($P < 0.0001$ for both groups; Mann–Whitney *U* test). Tumor attenuation of the *Min* phenotype was dose-dependent; $Apc^{Min/+};BLM^{T/T}$ mice developed significantly less adenomas than $Apc^{Min/+};BLM^{+/T}$ mice ($P = 0.016$; Mann–Whitney *U* test). Suppression of adenoma formation by *BLM-Tg* was most evident in the jejunal and ileac segments of the gastrointestinal tract (Fig. 1B), which is not surprising, as these regions comprise the predominant site of adenoma formation in the $Apc^{Min/+}$ mode (17). There was no difference in mean adenoma numbers between male and female mice. Adenomas were not observed in control groups of *BLM-Tg* or wild-type mice.

Despite the reduction in total adenomas by *BLM-Tg*, there was no significant reduction in the levels of GIN between groups (Fig. 1A), although the trend was suggestive. Compare means of 4.69 ± 4.22 for $Apc^{Min/+}$ to 2.71 ± 2.05 for $Apc^{Min/+};BLM^{+/T}$, and 3.00 ± 3.33 for $Apc^{Min/+};BLM^{T/T}$ mice. However, these sample sizes confer only a 30% power to detect differences between means of 1.56 with a significance level (α) of 0.05 (two-tailed). We would require 80 or more animals in each group to have 80% power to detect a difference between means of 1.34 with a significance level (α) of 0.05 (two-tailed).

BLM-Tg increases survival in the $Apc^{Min/+}$ mouse model of intestinal tumorigenesis

Survival of $Apc^{Min/+}$ mice was increased by the *BLM* transgene (Fig. 2). Median survival for $Apc^{Min/+}$ mice was 137 days compared with 196 days for $Apc^{Min/+};BLM^{+/T}$ mice and 221 days for $Apc^{Min/+};BLM^{T/T}$ mice ($P<0.0001$; log-rank test for both groups). Survival times between $Apc^{Min/+};BLM^{+/T}$ and $Apc^{Min/+};BLM^{T/T}$ mice were also significantly different ($P<0.0053$; log-rank test), indicating a dose-dependent effect of the transgene. Although *BLM-Tg* significantly extended survival of $Apc^{Min/+}$ mice, most likely due to reduced intestinal tumor burden, they died earlier than *BLM-Tg* litter mate controls, which are all still alive after 350 days (Fig. 2). It is not surprising that BLM overexpression was unable to mitigate the persistent intestinal tumorigenesis that is characteristic of the *Min* phenotype.

Transgenic BLM does not affect tumor etiology

While genetic background modifies tumor penetrance in the $Apc^{Min/+}$ model (21), adenomas rarely progress to carcinoma (22). Comparative histopathologic evaluation of intestinal lesions from $Apc^{Min/+};BLM^{+/T}$ and $Apc^{Min/+};BLT^{T/T}$ mice was consistent with the well-characterized etiology of tumor development in the $Apc^{Min/+}$ model (Fig. 3A–F; refs. 17, 20). Most adenomas were classified as low-grade; no adenocarcinomas were observed. Although more high-grade adenomas developed in $Apc^{Min/+}$ (10/282) compared with $Apc^{Min/+};BLM^{+/T}$ (1/148) or $Apc^{Min/+};BLM^{T/T}$ (1/101) mice, the numbers of adenomas assessed were insufficient to determine significance.

To more fully understand the nuanced effects of *Blm/BLM* dosage on tumor initiation versus progression in the $Apc^{Min/+}$ intestine, we employed the $Blm^{Cin/+}$ knockout mouse model (11). We examined tumors from aged $Apc^{Min/+};Blm^{Cin/+}$ mice ($n = 20$) to investigate how *Blm* haploinsufficiency affected tumor progression within the same intestinal model. Adenomas with high-grade dysplasia (Fig. 3G) were observed in 15 $Apc^{Min/+};Blm^{Cin/+}$ mice, and 4 mice also developed adenocarcinomas that invaded the serosa (Fig. 3H). There was a statistically significant increase in both carcinomas and high-grade dysplasia in the $Apc^{Min/+};Blm^{Cin/+}$ mice ($P < 0.0001$). These data suggest that *Blm/BLM* dosage can modulate tumor burden and progression in the

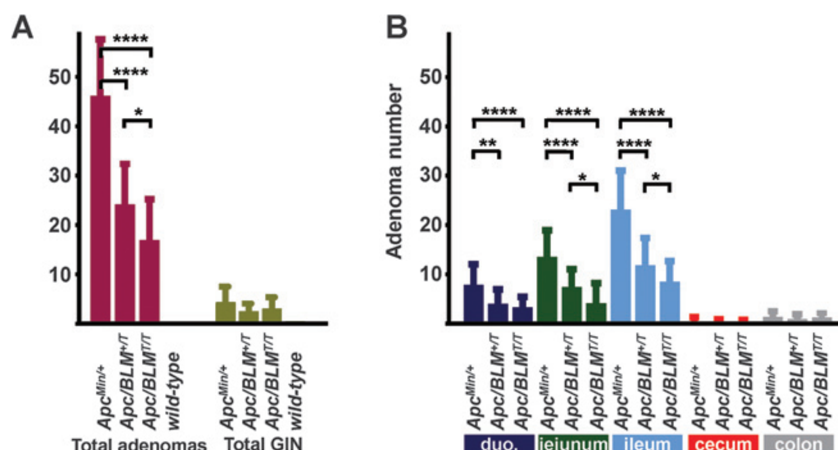

Figure 1.
Transgenic *BLM* suppresses adenoma formation in the $Apc^{Min/+}$ mouse model of intestinal tumorigenesis. A, total adenoma numbers and total levels of GIN for $Apc^{Min/+}$, $Apc^{Min/+};BLM^{+/T}$, $Apc^{Min/+};BLM^{T/T}$, and *BLM-Tg*/wild-type mice. Mean adenoma number ± SD and mean GIN ± SD was calculated for each genotype. Significant values are indicated above each bracket: *, $P < 0.02$; ****, $P < 0.0001$. B, the intestines of $Apc^{Min/+}$, $Apc^{Min/+};BLM^{+/T}$, and $Apc^{Min/+};BLM^{T/T}$ mice were dissected and divided into each intestinal compartment shown. Mean adenoma number ± SD was calculated for each tissue. Statistical analyses were performed using the Mann–Whitney *U* test. Significant values are indicated above each bracket: *, $P \leq 0.02$; **, $P < 0.002$; ****, $P < 0.0001$.

Downloaded from http://aacrjournals.org/cancerpreventionresearch/article-pdf/8/7/650/2254579/650.pdf by guest on 20 July 2024

Table 1. Mean number of intestinal adenomas per region in *Apc*$^{Min/+}$, *Apc*$^{Min/+}$;*BLM*$^{+/T}$, and *Apc*$^{Min/+}$;*BLM*$^{T/T}$ mice

Genotype	*n*	Intestinal region du.	je.	il.	ce.	co.	All tumors
Apc$^{Min/+}$	27	7.84	13.56	23.11	0.44	1.37	46.44
Apc$^{Min/+}$; *BLM*$^{+/T}$	18	4.00	7.44	11.83	0.28	0.94	24.44
Apc$^{Min/+}$; *BLM*$^{T/T}$	17	3.30	4.12	8.47	0.29	1.06	17.24
BLM-Tg & wild-type	22	0	0	0	0	0	0

Abbreviations: ce., cecum; co., colon; du., duodenum; il., ileum; je., jejunum.

mouse. Although *BLM-Tg* most likely suppresses adenoma formation by inhibiting progression from GIN to intestinal adenoma, it may also have subtle effects on the initiation of dysplasia that this study is not sufficiently powered to reveal.

Transgenic BLM does not attenuate intestinal tumor numbers in mismatch repair–deficient *Apc*$^{Min/+}$ mice

A well-documented aspect of the *Apc*$^{Min/+}$ phenotype on the *C57Bl-6J* background is that inactivation of the wild-type *Apc* locus by LOH is essential for subsequent intestinal adenoma formation (17). Given the known roles of *Blm/BLM* in HR, we investigated if our transgenic *BLM* could likewise reduce numbers of intestinal adenomas in an *Apc*$^{Min/+}$ model that was not dependent on LOH as a second-hit mechanism of inactivation. It has been observed that when *Apc*$^{Min/+}$ is combined with mismatch repair (MMR)–null mouse models, either *Mlh1*$^{-/-}$ or *Msh2*$^{-/-}$, the mechanism of *Apc* inactivation changes from that of LOH to intragenic mutation. Analyses of adenomas from *Mlh1*$^{-/-}$;*Apc*$^{Min/+}$ and *Msh2*$^{-/-}$;*Apc*$^{Min/+}$ mice demonstrated intragenic (point) mutation of the wild-type *Apc* allele in 81% and 85% of cases, respectively (23, 24). This shift is most likely due to the characteristic mutator phenotypes inherent to these specific models of MMR deficiency. Analyses of respective control groups of *Apc*$^{Min/+}$ mice from both of the above models confirmed LOH in all of the adenomas examined (23, 24).

We combined our *Apc*$^{Min/+}$;*BLM-Tg* model with the *Msh2*-null allele, *Msh2*$^{\Delta 7N}$ (19), and generated all possible combinations of *Apc*$^{Min/+}$;*BLM*^{T};*Msh2*$^{+/-}$ animals. Mice transgenic for *BLM* are collectively represented as *BLM*^{T}; they were not stratified as *BLM*$^{+/T}$ and *BLM*$^{T/T}$ for this analysis. The increased intestinal tumor burdens that developed in cohorts of *Apc*$^{Min/+}$;*BLM*^{T};*Msh2*$^{-/-}$ and *Apc*$^{Min/+}$;*Msh2*$^{-/-}$ mice resulted in a severe decline in animal survival, compelling necropsy of these groups at 11 to 12 weeks. Control groups of *Apc*$^{Min/+}$, *Apc*$^{Min/+}$;*BLM*^{T} and *Apc*$^{Min/+}$;*BLM*^{T};*Msh2*$^{+/-}$ mice were analyzed at the standard 16- to 17-week time point. Intestinal adenoma counts for the control groups were: *Apc*$^{Min/+}$, 49.5 ± 12.0; *Apc*$^{Min/+}$;*BLM*^{T}, 23.7 ± 8.9; and *Apc*$^{Min/+}$;*BLM*^{T};*Msh2*$^{+/-}$, 24.1 ± 10.3 (Fig. 4). Adenoma numbers for *Apc*$^{Min/+}$ and *Apc*$^{Min/+}$;*BLM*^{T} groups are similar to those of Fig. 1, indicating that introduction of the *Msh2*$^{\Delta 7N}$ allele onto the *Apc*$^{Min/+}$;*BLM*^{T} background did not alter tumor susceptibility in the intestine. It is also evident that heterozygosity for *Msh2* does not perturb adenoma development in the intestines of *Apc*$^{Min/+}$ mice which is consistent with published data (24, 25). The *Apc*$^{Min/+}$;*BLM*^{T};*Msh2*$^{-/-}$ and *Apc*$^{Min/+}$;*Msh2*$^{-/-}$ groups presented comparable adenoma counts of 272.0 ± 28.5 and 288.2 ± 32.3, respectively (Fig. 4). This striking increase in intestinal adenomas is a characteristic feature of MMR-deficient *Apc*$^{Min/+}$ mice phenotypes (23–26). Our data suggest that when Apc is inactivated by intragenic mutation in this model, rather than by LOH, transgenic BLM has no significant effect on the outcome of intestinal adenoma development.

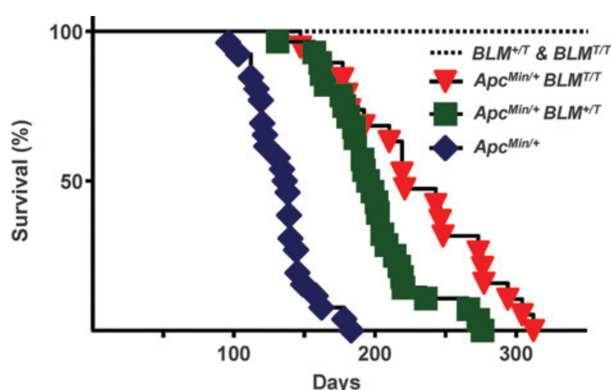

Figure 2.
Transgenic *BLM* increases survival in *Apc*$^{Min/+}$ mice. Groups of *BLM*$^{+/T}$ and/or *BLM*$^{T/T}$ ($n = 12$), *Apc*$^{Min/+}$ ($n = 26$), *Apc*$^{Min/+}$;*BLM*$^{+/T}$ ($n = 28$), and *Apc*$^{Min/+}$;*BLM*$^{T/T}$ ($n = 19$) mice were aged. Mice were observed on a daily basis for predetermined criteria necessitating removal and euthanasia. Kaplan–Meier plots were generated, and median survival times of each group were calculated. The log-rank test was used to determine the significance of differences in survival.

Overexpression of BLM modulates DNA repair by downregulating HR

Given the known role of *BLM* in maintaining genomic integrity (1, 2), we hypothesized that *BLM-Tg* ameliorated tumorigenesis in *Apc*$^{Min/+}$ mice by suppressing HR. To investigate this possible mechanism, *BLM-Tg* mice were crossed to the pink-eyed unstable (p^{un}) mouse model which measures *in vivo* HR levels. In this model, a somatic intrachromosomal deletion within the mouse *p* gene restores melanin production in the otherwise transparent cells of the retinal pigment epithelium (RPE), generating a clone of brown cells, or eye-spot (18). This deletion event occurs spontaneously and is dependent on HR. Thus, the number of RPE eye-spots represents an *in vivo* read-out for HR. Cohorts of $p^{un/un}$ and $p^{un/un}$;*BLM*^{T} mice were euthanized after 20 days, and RPE eye-spots were counted. Representative examples are shown in Fig. 5A and B. In contrast with *Apc*$^{Min/+}$ mice, *BLM-Tg* dosage does not appear to be a critical modifier in the $p^{un/un}$ model; differences in eye-spot numbers for $p^{un/un}$;*BLM*$^{+/T}$ and $p^{un/un}$;*BLM*$^{T/T}$ mice were not significant. Mitotic cell division is essentially complete in the RPE by P20 (27), so it is possible that the restricted developmental window of this tissue is insufficient to highlight subtle differences in HR between $p^{un/un}$;*BLM*$^{+/T}$ and $p^{un/un}$;*BLM*$^{T/T}$ genotypes. Therefore, these mice were combined and analyzed as one group (Fig. 5C). The number of eye-spots in control $p^{un/un}$ mice of 6.9 ± 3.2 is comparable with previous reports (18, 28), whereas BLM overexpression reduces HR 2-fold, resulting in 3.4 ± 1.9 eye-spots per RPE in $p^{un/un}$;*BLM*^{T} mice ($P < 0.0001$; Mann–Whitney *U* test). Although it was not possible to directly measure HR in the intestinal epithelial compartment of

Downloaded from http://aacrjournals.org/cancerpreventionresearch/article-pdf/8/7/650/2254579/650.pdf by guest on 20 July 2024

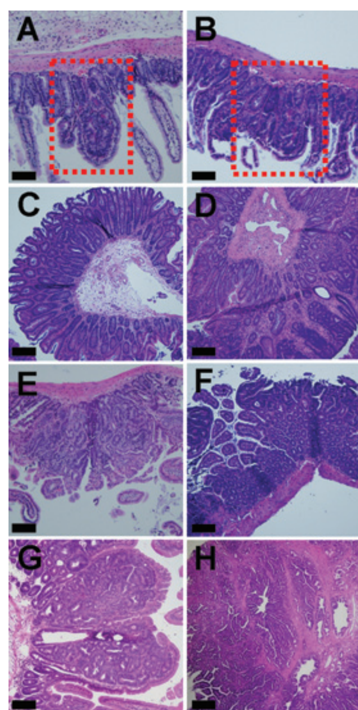

Figure 3.
Histopathology of intestinal tumor development associated with *Blm/BLM* in $Apc^{Min/+}$ mice. A–F, although *BLM-Tg* reduces adenoma numbers on the $Apc^{Min/+}$ background, it does not alter the underlying histopathology of emerging adenomas: A, $Apc^{Min/+}$ jejunum, boxed area highlights GIN; B, $Apc^{Min/+};BLM^{T/T}$ jejunum, boxed area highlights GIN; C, $Apc^{Min/+};BLM^{T/T}$ cecum, adenoma; D, $Apc^{Min/+};BLM^{+/T}$ colon, adenoma; E, $Apc^{Min/+};BLM^{+/T}$ jejunum, adenoma; F, $Apc^{Min/+};BLM^{T/T}$ ileum, adenoma. G–H, *Blm* haploinsufficiency drives tumor development and accelerates the development of intestinal adenomas with high-grade dysplasia and invasive carcinoma: G, $Apc^{Min/+};Blm^{Cin/+}$, adenoma with high-grade dysplasia; H, $Apc^{Min/+};Blm^{Cin/+}$, invasive adenocarcinoma. All sections were stained with hematoxylin and eosin. Scale bars each represent 100 μm.

our intestinal model, our data suggest that the observed reduction in adenoma numbers is also due to modulation of HR by *BLM-Tg*.

Discussion

Rescue of the $Blm^{Cin/Cin}$ embryonic lethal phenotype by *BLM-Tg* indicates that expression of this human ortholog is sufficiently regulated, within the physiologic context of our model, to direct normal development in *Blm*-null mice. Our findings that *BLM-Tg* reduces adenoma numbers in the $Apc^{Min/+}$ mouse model of intestinal tumorigenesis (Fig. 1) are consistent with the known role of *BLM* in HR and its requirement for maintaining genomic integrity (2, 11). Moreover, BLM-Tg expression suppressed adenoma formation in the $Apc^{Min/+}$ model by a dose-dependent mechanism (Fig. 1), suggesting that augmentation of the HR pathway may be a viable objective for attenuating tumor suppression in specific *in vivo* milieus, notably the intestinal compartment. Reduction of intestinal tumor burden results in accompanying dose-dependent increases in median survival times for $Apc^{Min/+};BLM^{+/T}$ and $Apc^{Min/+};BLM^{T/T}$ mice (Fig. 2).

Adenomas that developed in $Apc^{Min/+};BLM^{+/T}$ mice were pathologically identical to those from $Apc^{Min/+}$ animals (Fig. 3), indicating that the *BLM-Tg* did not affect tumor origin or skew tumor spectrum in this intestinal model. Furthermore, long-term expression does not adversely alter the wild-type phenotype of $BLM^{+/T}$ and $BLM^{T/T}$ mice. Mice ($n = 12$) have now been aged for over 24 months without deleterious effects on survival or overt signs of tumorigenesis. This is somewhat surprising because data from the p^{un} model indicate that, mechanistically, BLM-Tg overexpression downregulates HR 2-fold (Fig. 5). However, given the crucial function of HR in mediating error-free repair of DNA damage, it is possible that aging *BLM-Tg* mice may ultimately prove more susceptible to spontaneous tumorigenesis. Perhaps if aged mice were challenged with radiomimetic agents, the inflicted DNA damage might exceed their (lowered) threshold for HR repair, consequently resulting in an increased susceptibility to tumorigenesis. Transgenic mouse lines have also been generated for *Wrn*, another member of the RecQ helicase family (29). Although the wild-type *Wrn* transgene has yet to be tested in models of tumorigenesis, it has no effect on HR in RPE cells of the p^{un} mouse (30).

The elevated BLM levels observed in our $Apc^{Min/+};BLM\text{-}Tg$ model most likely reduce adenoma formation through suppression of HR, thus maintaining heterozygosity of the wild-type *Apc* allele. We used the p^{un} and MMR-deficient $Msh2^{-/-}$ models to further investigate the mechanism of tumor reduction in the $Apc^{Min/+};BLM^{T}$ mice, rather than attempting to correlate a reduction in surrogate markers of HR, such as Rad51 foci, with reduction in adenoma burden. These genetic models presented a more relevant system for assessing the effects of the *BLM-Tg* on HR *in vivo*. A 2-fold reduction of eye-spots in RPE cells of $p^{un/un};BLM^{T}$ mice (Fig. 5) suggests that *BLM-Tg* directly modulates HR in this tissue. Our interpretation of the observed reduction in adenoma numbers in the $Apc^{Min/+};BLM^{T}$ model is that it is caused by the effect of *BLM-Tg* on HR in the intestinal epithelia, thus suppressing LOH of the wild-type *Apc* allele. This conclusion is supported by the data from the $Apc^{Min/+};BLM^{T};Msh2^{-/-}$ mice. When *Apc* is activated by point mutation, due to innate MMR deficiency, thus precluding the requirement for inactivation of the wild-type *Apc* allele by LOH, there are no observable differences in intestinal adenoma numbers between $Apc^{Min/+};BLM^{T};Msh2^{-/-}$

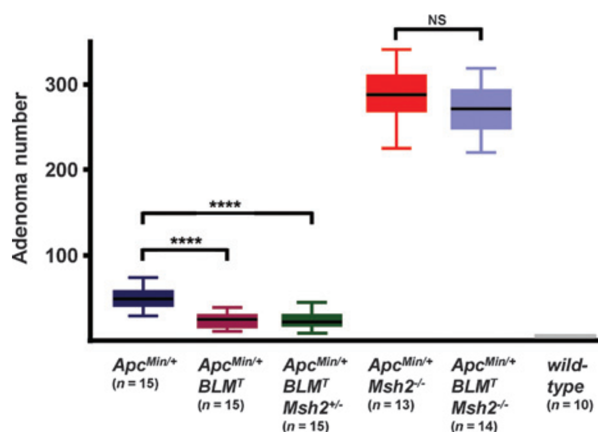

Figure 4.
Transgenic BLM does not attenuate intestinal tumor numbers in MMR-deficient $Apc^{Min/+}$ mice. Box and whiskers plot showing total adenoma numbers arising in $Apc^{Min/+}$ and $Apc^{Min/+};BLM^{T}$ mice on *Msh2*-deficient backgrounds. Significant values are indicated above each bracket: ****, $P < 0.0001$; NS, not significant. Statistical analyses were performed using the Mann–Whitney *U* test.

Downloaded from http://aacrjournals.org/cancerpreventionresearch/article-pdf/8/7/650/2254579/650.pdf by guest on 20 July 2024

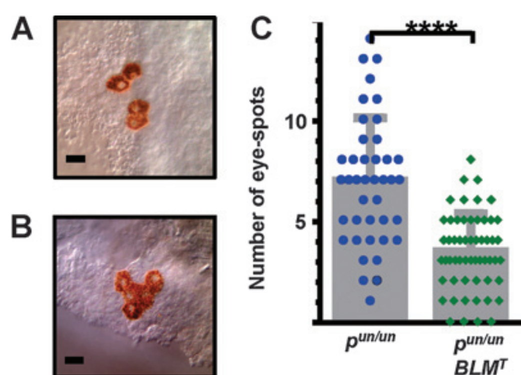

Figure 5.
Expression of *BLM-Tg* downregulates HR in the p^{un} mouse RPE. Eye-spots consist of pigmented clones of revertant RPE cells in which melanin production has been restored by an intrachromosomal recombination event. They are easily visible on the transparent RPE background. A and B, representative examples of eye-spots in $p^{un/un}$;BLM^T mice. These are comprised of: A, single or simple multiples of revertant RPE cells although (B) sometimes rarer, more complex configurations are observed. Eye-spots separated by a single nonrevertant (clear) cell are scored as a single unit. C, *BLM-Tg* suppresses HR in p^{un} RPE cells. $p^{un/un}$;$BLM^{+/T}$ and $p^{un/un}$;$BLM^{T/T}$ mice have been combined and represented as a single group, $p^{un/un}$;BLM^T, because analyses demonstrated both genotypes are similarly effective in this model. Mean ± SD are shown for each group. $p^{un/un}$ mice have 6.9 ± 3.2 eye-spots, $n = 277$, 40 RPE; $p^{un/un}$;BLM^T mice have 3.4 ± 1.9 eye-spots, $n = 192$, RPE = 56. Statistical analyses were performed using the Mann–Whitney *U* test; ****, $P < 0.0001$. Scale bars each represent 50 μm.

and $Apc^{Min/+}$;$Msh2^{-/-}$ mice (Fig. 4). If *BLM-Tg* was affecting adenoma formation through other mechanisms unrelated to HR, one would predict that adenoma numbers should still differ between these two models. This is not the case.

Consistent with this model, levels of GIN are also reduced between $Apc^{Min/+}$ and $Apc^{Min/+}$;*BLM-Tg* genotypes, although they do not meet statistical significance (Fig. 1A). If correct, *BLM-Tg* would act before the potential onset of GIN, since GIN pathologically precedes adenomas in the $Apc^{Min/+}$ model and since LOH of the wild-type *Apc* allele is a fundamental requirement for GIN development on a *C57Bl-6J* background (31). In addition to perturbing LOH, and hence subsequent levels of GIN and adenomas, it is possible that *BLM-Tg* may selectively target neoplastic cells after they have emerged as larger lesions on the $Apc^{Min/+}$ background. It remains unclear whether elevating BLM levels could eliminate, perhaps through apoptosis, single or small populations of nascent cells that have acquired two mutant alleles of *Apc*.

Data from our $Apc^{Min/+}$;BLM^T models suggest that levels of specific DNA repair proteins may be titrated to achieve positive therapeutic outcomes in the context of specific hereditary cancer syndromes, exemplified by FAP. There are many inhibitors readily available that target the HR repair pathway and downregulate HR (reviewed in refs. 32, 33). However, we are unaware of any small-molecule inhibitors, or other reagents, that effect upregulation of endogenous *BLM* and thus, might prove more suitable for therapeutic applications. With this in mind, we are investigating expression profiles of our *BLM-Tg* model to determine if there are other molecular targets that are more amenable to therapeutic modulation.

Our study establishes that BLM expression can be effectively manipulated in a mouse model of intestinal tumorigenesis to successfully attenuate the tumor phenotype. We show that overexpression of human *BLM* reduces intestinal adenoma formation in the $Apc^{Min/+}$ mouse model and propose that the mechanism is through downregulation of the HR repair pathway. This presents the potential to explore new avenues for intestinal tumor prevention by controlling levels of BLM expression or other genes of the DNA repair pathways. Our data demonstrate the therapeutic potential of titrating levels of specific DNA repair proteins that may be protective against tumor formation and suggest that this approach of modulating fundamental DNA repair pathways may be a viable pharmacologic strategy for cancer prevention.

Disclosure of Potential Conflicts of Interest

No potential conflicts of interest were disclosed.

Disclaimer

The content is solely the responsibility of the authors and does not necessarily represent the official views of the National Center for Advancing Translational Sciences or the NIH. The funders had no role in study design, data collection and analysis, decision to publish, or preparation of the article.

Authors' Contributions

Conception and design: M.A. McIlhatton, G.P. Boivin, J. Groden
Development of methodology: M.A. McIlhatton, G.P. Boivin
Acquisition of data (provided animals, acquired and managed patients, provided facilities, etc.): K. Murnan, G.P. Boivin, J. Groden
Analysis and interpretation of data (e.g., statistical analysis, biostatistics, computational analysis): M.A. McIlhatton, K. Murnan, G.P. Boivin, J. Groden
Writing, review, and/or revision of the manuscript: M.A. McIlhatton, G.P. Boivin, J. Groden
Administrative, technical, or material support (i.e., reporting or organizing data, constructing databases): C.M. Croce
Study supervision: M.A. McIlhatton, J. Groden
Other (generated BLM transgene for the BLM transgenic mouse used in the study): D. Carson

Acknowledgments

The authors acknowledge support from the Bloom's Syndrome Foundation and The Solid Tumor Biology Program in the OSU Comprehensive Cancer Center (to J. Groden).

Grant Support

This work was supported by NIH grants CA117898 (to J. Groden), CA63507 (to J. Groden), CA152758 (to C.M. Croce), and CA166905 (to C.M. Croce). The project was supported by awards 8UL1TR000090-05, 8KL2TR000112-05, and 8TL1TR000091-05 from the National Center for Advancing Translational Sciences (to J. Groden). K. Murnan was supported by the Pelotonia Fellowship Program.

The costs of publication of this article were defrayed in part by the payment of page charges. This article must therefore be hereby marked *advertisement* in accordance with 18 U.S.C. Section 1734 solely to indicate this fact.

Received January 9, 2015; revised March 27, 2015; accepted April 7, 2015; published OnlineFirst April 23, 2015.

References

1. Chu WK, Hickson ID. RecQ helicases: multifunctional genome caretakers. Nat Rev Cancer 2009;9:644–54.
2. Risinger MA, Groden J. Crosslinks and crosstalk: human cancer syndromes and DNA repair defects. Cancer Cell 2004;6:539–45.

Downloaded from http://aacrjournals.org/cancerpreventionresearch/article-pdf/8/7/650/2254579/650.pdf by guest on 20 July 2024

3. Karow JK, Chakraverty RK, Hickson ID. The Bloom's syndrome gene product is a 3′-5′ DNA helicase. J Biol Chem 1997;272:30611–14.
4. Ellis NA, Groden J, Ye TZ, Straughen J, Lennon DJ, Ciocci S, et al. The Bloom's syndrome gene product is homologous to RecQ helicases. Cell 1995;83:655–66.
5. German J, Archibald R, Bloom D. Chromosomal breakage in a rare and probably genetically determined syndrome of Man. Science 1965; 148:506–7.
6. Braybrooke JP, Li J-L, Wu L, Caple F, Benson FE, Hickson ID. Functional interaction between the Bloom's syndrome helicase and the RAD51 paralog, RAD51L3 (RAD51D). J Biol Chem 2003;278:48357–66.
7. Bugreev DV, Yu X, Egelman EH, Mazin AV. Novel pro- and anti-recombination activities of the Bloom's syndrome helicase. Genes Dev 2007; 21:3085–94.
8. Chaganti RS, Schonberg S, German JA. A manyfold increase in sister chromatid exchanges in Bloom's syndrome lymphocytes. Proc Natl Acad Sci U S A 1974;71:4508–12.
9. German J, Sanz MM, Ciocci S, Ye TZ, Ellis NA. Syndrome-causing mutations of the BLM gene in persons in the Bloom's Syndrome Registry. Hum Mutat 2007;28:743–53.
10. Luo G, Santoro IM, McDaniel LD, Nishijima I, Mills M, Youssoufian H, et al. Cancer predisposition caused by elevated mitotic recombination in Bloom mice. Nat Genet 2000;26:424–9.
11. Goss KH, Risinger MA, Kordich JJ, Sanz MM, Straughen JE, Slovek LE, et al. Enhanced tumor formation in mice heterozygous for Blm mutation. Science 2002;297:2051–3.
12. McDaniel LD, Chester N, Watson M, Borowsky AD, Leder P, Schultz RA. Chromosome instability and tumor predisposition inversely correlate with BLM protein levels. DNA Repair 2003;2:1387–1404.
13. Gruber SB, Ellis NA, Scott KK, lmog R, Kolachana P, Bonner JD. BLM heterozygosity and the risk of colorectal cancer. Science 2002;297:2013.
14. Fearon ER. Molecular genetics of colorectal cancer. Annu Rev Pathol 2011;6:479–507.
15. Groden J, Thliveris A, Samowitz W, Carlson M, Gelbert L, Albertsen H, et al. Identification and characterization of the familial adenomatous polyposis coli gene. Cell 1991;66:589–600.
16. Albuquerque C, Breukel C, van der Luijt R, Fidalgo P, Lage P, Slors FJ, et al. The `just-right' signaling model: APC somatic mutations are selected based on a specific level of activation of the beta-catenin signaling cascade. Hum Mol Genet 2002;11:1549–60.
17. Shoemaker AR, Gould KA, Luongo C, Moser AR, Dove WF. Studies of neoplasia in the Min mouse. Biochim Biophys Acta 1997;1332:F25–48.
18. Brown AD, Claybon AB, Bishop AJ. A conditional mouse model for measuring the frequency of homologous recombination events in vivo in the absence of essential genes. Mol Cell Biol 2011;31:3593–602.
19. Smits R, Hofland N, Edelmann W, Geugien M, Jagmohan-Changur S, Albuquerque C, et al. Somatic Apc mutations are selected upon their capacity to inactivate the beta-catenin downregulating activity. Genes Chrom Can 2000;29:229–39.
20. Boivin GP, Washington K, Yang K, Ward JM, Pretlow TP, Russell R. Pathology of mouse models of intestinal cancer: consensus report and recommendations. Gastroenterology 2003;124:762–77.
21. Shoemaker AR, Moser AR, Midgley CA, Clipson L, Newton MA, Dove WF. A resistant genetic background leading to incomplete penetrance of intestinal neoplasia and reduced loss of heterozygosity in ApcMin/+mice. Proc Natl Acad Sci U S A 1998;95:10826–31.
22. Halberg RB, Waggoner J, Rasmussen K, White A, Clipson L, Prunuske AJ, et al. Long-lived Min mice develop advanced intestinal cancers through a genetically conservative pathway. Cancer Res 2009;69: 5768–75.
23. Shoemaker AR, Haigis KM, Baker SM, Dudley S, Liskay RM, Dove WF. Mlh1 deficiency enhances several phenotypes of Apc(Min)/+ mice. Oncogene 2000;19:2774–9.
24. Reitmair AH, Cai JC, Bjerknes M, Redston M, Cheng H, Pind MT, et al. MSH2 deficiency contributes to accelerated APC-mediated intestinal tumorigenesis. Cancer Res 1996;56:2922–6.
25. Lal G, Ash C, Hay K, Redston M, Kwong E, Hancock B, et al. Suppression of intestinal polyps in Msh2-deficient and non-Msh2-deficient multiple intestinal neoplasia mice by a specific cyclooxygenase-2 inhibitor and by a dual cyclooxygenase-1/2 inhibitor. Cancer Res 2001;61:6131–6.
26. Belcheva A, Green B, Weiss A, Streutker C, Martin A. Elevated incidence of polyp formation in $APC^{Min/+}Msh2^{-/-}$ mice is independent of nitric oxide-induced DNA mutations. PLoS One 2013;8:e65204.
27. Bodenstein L, Sidman RL. Growth and development of the mouse retinal pigment epithelium. I. Cell and tissue morphometrics and topography of mitotic activity. Dev Biol 1987;121:192–204.
28. Bishop AJ, Hollander MC, Kosaras B, Sidman RL, Fornace AJ Jr, Schiestl RH. Atm-, p53- and Gadd45a-deficient mice show an increased frequency of homologous recombination at different stages during development. Cancer Res 2003;63:5335–43.
29. Wang L, Ogburn CE, Ware CB, Ladiges WC, Youssoufian H, Martin GM, et al. Cellular Werner phenotypes in mice expressing a putative dominant-negative human WRN gene. Genetics 2000;154:357–62.
30. Yamamoto ML, Reliene R, Oshima J, Schiestl RH. Effects of human Werner helicase on intrachromosomal homologous recombination mediated DNA deletions in mice. Mutat Res 2008;644:11–6.
31. Paulsen JE, Steffensen IL, Løberg EM, Husøy T, Namork E, Alexander J. Qualitative and quantitative relationship between dysplastic aberrant crypt foci and tumorigenesis in the Min/+ mouse colon. Cancer Res 2001;61:5010–5.
32. Carvalho JF, Kanaar R. Targeting homologous recombination-mediated DNA repair in cancer. Expert Opin Ther Targets 2014;18:427–58.
33. Huang F, Mazin AV. Targeting the homologous recombination pathway by small molecule modulators. Bioorg Med Chem Lett 2014;24:3006–13.

Downloaded from http://aacrjournals.org/cancerpreventionresearch/article-pdf/8/7/650/2254579/650.pdf by guest on 20 July 2024